Mass Spectrometry & Purification Techniques

Mezghich et al., Mass Spectrom Purif Tech 2017, 3:1
DOI: 10.4172/2469-9861.1000118

Research Article Open Access

Photochemical Degradation of the Antimicrobial Sulfamethoxazole upon Solar Light Excitation: Kinetics and Elucidation of Byproducts Using LC/ESI+/MS2 Technique

Soumaya Mezghich[1,2], Fadhila Ayari[2] and Mohamed Sarakha[1]*

[1]Université Clermont Auvergne, Institut de Chimie de Clermont-Ferrand (ICCF), CNRS, BP 10448, F-63000 Clermont-Ferrand, France
[2]Université de Carthage, Faculté des Sciences de Bizerte, LACReSNE, Zarzouna, Bizerte 7021, Tunisia

Abstract

The fate of the antimicrobial compounds in the environment is of great interest since their presence in the aquatic systems has raised environmental problems. More and more chemicals of this class are treated as emerging contaminants. The degradation of these compounds may result in the formation of a wide array of metabolites which can be more toxic than the parent substrate. Therefore, precise elucidation of all possible transformation products as well as a thorough study of their physico-chemical and biological properties is of great importance. The present work deals with the study of the photochemical behavior of sulfamethoxazole from the kinetic aspect as well as the elucidation of the products arising from the solar irradiation of the antimicrobial sulfamethoxazole in the aqueous solutions. HPLC/MS and HPLC/MS/MS with accurate mass measurements were used for this purpose.

Keywords: Sulfamethoxazole; Photolysis; Antimicrobial; HPLC/MS

Introduction

Compounds such as pharmaceuticals, industrial chemicals, pesticides, dyes, UV-filters are more and more introduced into the environment owing to the intense human activities [1-6]. The resulting undesired ecological consequences are associated with their persistence in the various environmental media, namely surface waters, ground waters, soil and even the atmosphere. Thus, the interest in these environmental effects leads to an increase of the research activities that permit the study of the fate of such pollutants. Among the processes that contribute in the degradation of these pollutants, photochemical reaction through solar excitation may play an important role [7,8]. Such action of light permits the degradation of the pollutants and also the formation of metabolites which may present toxicity higher that of the parent compound [9-11].

Among these pollutants, the antimicrobial sulfamethoxazole is largely used [12-14] and it is of great interest to study its fate into the environment because of its potential negative effect. Such compound has been found in aquatic media owing to the inefficient elimination during sewage treatment and has been shown to significantly absorb solar light [15-17]. Some studies were devoted to the elimination of sulfamethoxazole using various photocatalytic systems [18] and permit its entire elimination. The aim of the present work is to study its fate in aqueous solution through light excitation and more particularly to elucidate the nature of their metabolites.

Experimental Part

2-Sulfanilamidothiazole or Sulfamethoxazole (CAS number 71-14-0) was obtained from Sigma Aldrich and used as received. Except when stated, all the other reagents were of the purest grade commercially available and were used without further purification. All the solutions were with deionised ultrapure water that was purified with Milli-Q devise (Millipore) and its purity was controlled by its resistivity. pH measurements were carried out with a JENWAY 3310. The ionic strength was not controlled.

The irradiation system was a device that simulates solar radiation (Suntest-CPS+, Atlas) equipped with a xenon lamp and a filter that permits the transmission wavelength above 290 nm. The power was fixed to provide about 550 $W.m^{-2}$ and samples temperature was controlled by a water flow (T= 20°C). A cylinder reactor made in stainless steel equipped with two germicidal lamps (Mazda T815 15W) emitting selectively at 254 nm and symmetrically installed around the cylinder were used. The reactor, a quartz tube (d=2.5 cm) containing a maximum of 50 mL solution, was located in the centre of the container.

The disappearance of the antimicrobial and the formation of the products were followed by high performance liquid chromatography using a Waters 2695 HPLC (Alliance) chromatograph system equipped with a Waters 2998 photodiode array detector. The experiments were performed by UV detection at either 250 nm or 280 nm and by using a reverse phase Nucleodur column (Macherey-Nagel, 100-5 C18 ec; 150–4.6 mm). The flow rate was 1.0 mL min^{-1} and the injected volume was 50 µL. The elution was accomplished with water, formic acid (0.1%) and acetonitrile (60/40 v/v). A Waters/Micromass LC/QTOF tandem mass spectrometer (Micromass, Manchester, UK), with an orthogonal geometry Z-spray ion source, was used for LC/ESI/MS and LC/ESI/MS/MS experiments. LC separation was performed using the gradient program reported in the literature [19]. Eluate was subjected to electrospray ionization (ESI) in the positive ion as well as negative mode and resulted in the formation of protonated molecules and deprotonation of the sample components. Scanning was performed in the range between m/z 60 and 600. The elemental composition of the recorded ions was further determined using MassLynx Elemental Composition software V4.1 (Micromass). C, H, N, O and S were selected as possible elements present. In LC/MS analyses, in order to assign the elemental formulas, the minimum and maximum atoms of each element were set as follows: C from 1 to 20; H from 1 to 20; N from 0 to 5; O from 0 to 10 and S from 0 to 2. No nitrogen rule, ring and double bond equivalents were applied. The maximum deviation was set to 10 ppm. Five scans were combined before the integration of the

***Corresponding author:** Mohamed Sarakha, Université Clermont Auvergne, Institut de Chimie de Clermont-Ferrand (ICCF), CNRS, BP 10448, F-63000 Clermont-Ferrand, France, Tel: +330473407170; E-mail: mohamed.sarakha@uca.fr

Received June 05, 2017; **Accepted** June 12, 2017; **Published** June 16, 2016

Citation: Mezghich S, Ayari F, Sarakha M (2017) Photochemical Degradation of the Antimicrobial Sulfamethoxazole upon Solar Light Excitation: Kinetics and Elucidation of Byproducts Using LC/ESI+/MS2 Technique. Mass Spectrom Purif Tech 3: 118. doi:10.4172/2469-9861.1000118

individual peaks. The desolvation and ion source temperatures were set at 250°C and 100°C, respectively. Nitrogen was used as the nebulizer (35 L/h) as well as a desolvation gas (350 L/h). The optimized voltages for the probe and ion source components (to produce maximum intensity) were 3 kV for the stainless-steel capillary, 35 V for the sample cone and 1 V for the extractor cone. The sampling rate of approximately 20 scans s^{-1}.

Tandem mass spectrometric (MS/MS) experiments in collisionally induced dissociation (CID) mode were performed using argon in the collision cell at a pressure of 4.0×10^{-3} mbar. A collision energy gradient (15-35 V) was used for preliminary fingerprints and specific energies were then used to unambiguously assign the product ions. The $[M+H]^+$ or $[M-H]^-$ precursor ions were used as a lock mass for the MS/MS experiments and allowed for accurate mass measurements to be undertaken. The ion formulae were determined by restricting the possible elements present to those in the precursor ion formulae, and setting the maximum allowed deviation in the mass measurements to 20 ppm. UV-visible spectra were recorded with a Cary 3 double beam spectrophotometer.

Results and Discussion

Kinetic studies

The UV absorption spectrum of the antimicrobial sulfamethoxazole **(STZ)** exhibits a well defined absorption band with a maximum at 262 nm and with an absorption molar coefficient of 11400 mol^{-1} L cm^{-1} (Figure 1A). Such electronic transition is more likely owing to a π–π* transition of the aniline part of the molecule. There is no evidence of a n-π* band that is probably hidden by the intense π–π* electronic transition.

It is of great importance to note that such absorption extends to 320 nm that clearly indicates that sulfamethoxazole may be involved in photochemical processes upon direct solar light excitation. The evolution of the absorption at 266 nm at various pH values permitted the determination of the pKa values. As clearly shown in Figure 1B, two different pKa's were obtained; pKa_1=1,82 ± 0,06 et pKa_2=5,60 ± 0,05. They correspond to the following protolytic equilibria (Scheme 1).

The photochemical behavior of sulfamethoxazole at a concentration of $(1.0 \times 10^{-4}$ mol L^{-1}; pH =5.3) was studied upon excitation with a suntest setup as well as with a monochromatic light at 254 nm, 290 nm and 310 nm. Under all these different conditions, **STZ** undergoes a degradation process as clearly demonstrated by the important evolution of the characteristic UV absorption spectrum (Figure 2) when a monochromatic light at 254 nm was used. Two well defined isobestic points were observed at 250 nm and 290 nm. It is worth noting that no thermal degradation was detected when **STZ** was kept in the dark and room temperature for a period of 24 hours. By assuming that within the first stages of the irradiation that the absorption is mainly due to **STZ**, a first order rate constant may be determined. Under our experimental conditions, this was evaluated to 4.6×10^{-3} min^{-1} in aerated medium and by excitation at 254 nm. The quantum yield for **STZ** disappearance was determined under various oxygen concentrations, namely aerated, oxygenated and deoxygenated conditions. It was evaluated to 0.11, 0.15 and 0.08 respectively. Such result clearly indicates that dissolved molecular oxygen plays an important role in the **STZ** photochemical process and appears to enhance its degradation.

It should also be noted that an increase of the absorbance was also observed in wavelength region 350-800 nm of the spectrum indicating the formation of colored byproducts. These products, that are more likely due to oxidized oligomeric species, appear to be instable under our experimental conditions and disappear thermally making their elucidation difficult.

Analytical studies

HPLC analysis of an irradiated solution of **STZ** shows, after 35% conversion, the formation of several byproducts. They were all produced from the early stages of the irradiation and detected using DAD and HPLC/MS through ESI+ and ESI- modes. Even though these products were not well separated, they were tentatively elucidated using HPLC/MS/MS technique. As clearly indicated in Figure 3, all the byproducts present retention times lower than that of the parent compound **STZ** (10.3 min) indicating that we are dealing with small molecules or/and more polar compounds. The main products were labeled in the order of their retention times from **P1** to **P5** (Table 1).

Table 1 gathers all the features and results for the main products under ESI+ analyses. The findings were further confirmed by ESI- mode. Under our experimental conditions, the elemental composition was selected when the difference between the accurate mass and the calculated mass was lower than 10 ppm.

As clearly shown from their elemental compositions, products **P1** with 6 carbon atoms and **P2** with 4 carbon atoms are the results of some photochemical scission that occurs on the starting compound. They were easily identified as sulfanilic acid (**P1**) and 3-amino-5-methylisoxazole (**P2**) and their formation arises from the photohydrolysis reaction of

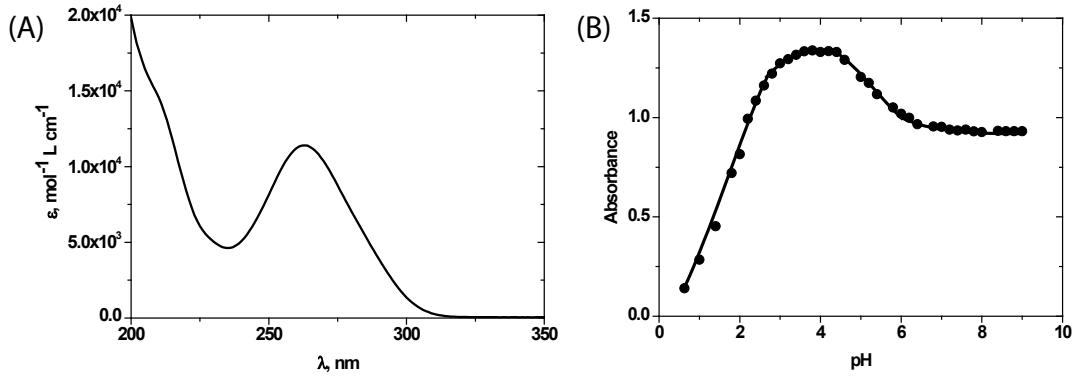

Figure 1: (A) Absorption spectrum of sulfamethoxazole **(STZ)** at a concentration of 1.0×10^{-4} mol L^{-1} and at a pH of 5.4. (B) Evolution of the absorbance at λ=266 nm as a function of pH.

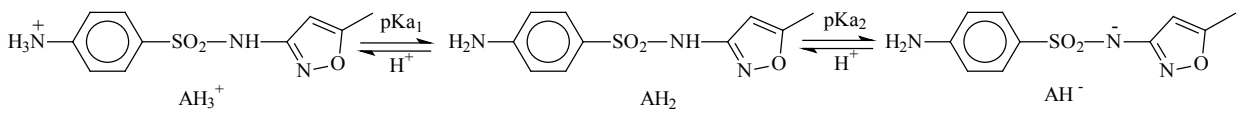

Scheme 1: Protolytic equilibria.

Retention time minutes	Product	m/z [M+H+]	Accurate mass	Elemental composition	Calculated mass	Error (ppm)
2.0	**P1**	174	174.0239	$C_6H_8NO_3S^+$	174.0225	+8.1
2.5	**P2**	99	99.0565	$C_4H_7N_2O^+$	99.0558	+6.7
3.7	**P3**	190	190.0992	$C_{10}H_{12}N_3O^+$	190.0980	+6.1
5.4	**P4**	254	254.0578	$C_{10}H_{12}N_3O_3S^+$	254.0599	-8.4
9.7	**P5**	270	270.0557	$C_{10}H_{12}N_3O_4S^+$	270.0548	+3.1
10.3	**STZ**	254	254.0591	$C_{10}H_{12}N_3O_3S^+$	254.0599	-3.3

Table 1: Accurate, exact masses and elemental compositions for the by-products P_1 to P_4 and **STZ** as obtained by LC/MS in ESI+ mode.

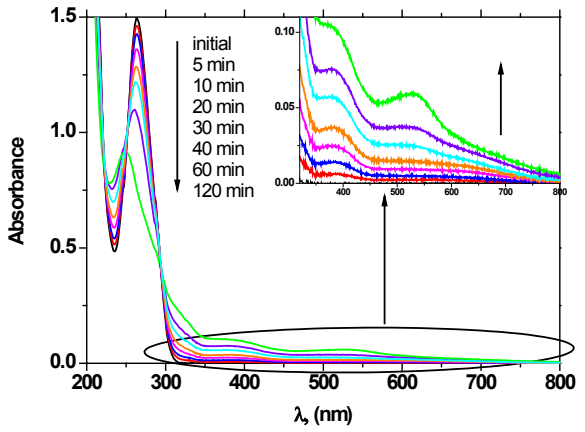

Figure 2: UV absorption spectrum evolution of an aerated solution of **STZ** (1.0×10^{-4} mol L^{-1}; pH=5.3) upon excitation at 254 nm.

the sulfamethoxazole according to the following process (Scheme 2).

The other three byproducts which conserve the number of carbon atoms are oxidized (**P5**), isomer (**P4**) and desulfonated (**P3**) products. In order to determine their precise chemical structure we undertook experiments by HPLC/MS/MS and we deeply analyzed their fragmentation process. As a first step and prior to the precise elucidation of the product structures, we undertook a close interpretation of the fragmentation process of the starting compound, **STZ.**

CID analyses of sulfamethoxazole, STZ: The CID spectrum of **STZ** shows that an efficient fragmentation of the precursors $[M+H]^+$ (m/z=254) occurs under a collision energy of 20 eV (Figure 4). It is dominated by four intense fragment ions at m/z=156(**d**), 108(**f**), 99(**g**), 93(**h**) and 92(**i**) together with several and relatively minor fragment ions at m/z=236(**a**), 188(**b**), 160(**c**) and 147(**e**). Their elemental compositions were obtained with the help of MassLynx V4.1 software through the determination of their accurate masses and were conserved when the error was lower than 20 ppm (Table 2).

Since the chemical structure of **STZ** presents several protonation sites, namely S and O on the SO_2 function as well as NH parts, we studied the fragmentation on the basis of these sites. The fragment ion **a**, with the elemental composition $\mathbf{C_{10}H_{10}N_3O_2S^+}$ (error of +6.0 ppm), arises from the protonation of oxygen at the SO_2 part and the elimination of water molecule with the help of the adjacent NH moiety. The resulted fragment undergoes a SO elimination leading to the formation of fragment **b** (m/z=188, $\mathbf{C_{10}H_{10}N_3O^+}$, error of -7.9 ppm) (Scheme 3).

The protonation at the nitrogen atom on the -SO_2-NH- part gives rise to the formation of the fragment ion **d** (m/z=156, $\mathbf{C_6H_6NO_2S^+}$) through the heterolytic scission of the S-N bond. The generated fragment ion **d** may lose sulfur dioxide permitting the formation of fragment **i** (m/z=92, $\mathbf{C_6H_6N^+}$) or sulfur monoxide leading to fragment **f** (m/z=108, $\mathbf{C_6H_6NO^+}$, **error=-7.8 ppm**). The formation of fragment g (m/z=99, $\mathbf{C_4H_7N_2O^+}$) proceeds through the same protonation followed by an intramolecular rearrangement as described in the following Scheme (Scheme 4).

The generation of fragment ion **h** (m/z=93, $\mathbf{C_6H_5O^+}$, **error=-17.6 ppm**) could involve the previous generated fragment **d.** This will involve an intramolecular hydrogen transfer from amine group to the SO_2 group followed by the loss of neutral NH=S=O molecule according to the Scheme below (Scheme 5).

Both fragments **c** (m/z=160, $\mathbf{C_4H_6N_3O_2S^+}$) and **e** (m/z=147, $\mathbf{C_4H_7N_2O_2S^+}$) involves the protonation on the oxygen of SO_2 function followed by two different intramolecular rearrangements with first the elimination of phenol and second elimination of quinine monoamine neutral molecule (Scheme 6).

CID analyses of P5: The comparison the elemental composition of **P5** with of the starting compound (**STZ**) shows the addition of an oxygen atom on the chemical structure. The exact position of such atom may be deduced from the deep analysis of the ESI+/MS^2 spectra (Figure 5) and the comparison of the resulted CID with that of **STZ**.

As clearly shown by, the two CID spectra show several common fragment ions and some specific ones. It is clear from Table 3 that all the identified fragments that do not contain the phenyl structure in the **STZ** CID spectrum are also present in that of **P5**, namely m/z=99, 160 and 147 while those containing the phenyl part are also present with 16 units difference as obtained between **P5** and **STZ**. It should be noted that the fragments ion observed at m/z=108 is not really a common ion. Actually, the fragment ion m/z=92 in the **STZ** spectrum was converted to m/z=108 in the **P5** spectrum while the fragment m/z=108 in the **STZ** was converted to m/z=124 in the **P5** spectrum (Scheme 7).

Such observations are in favor of the addition of oxygen atom on the phenyl moiety as a hydroxyl group. Such substitution may be obtained photochemically by the formation first of a radical cation via electron ejection or photoionisation and second by the action

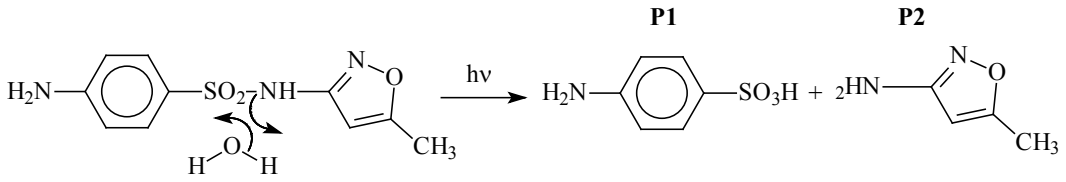

Scheme 2: Photohydrolysis reaction of the sulfamethoxazole.

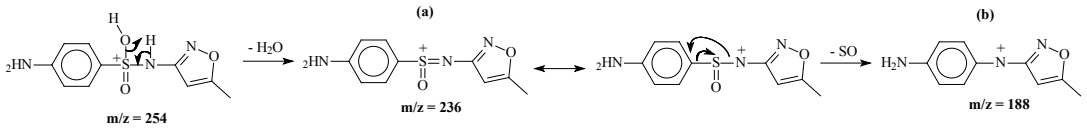

Scheme 3: SO elimination leading to the formation of fragment b.

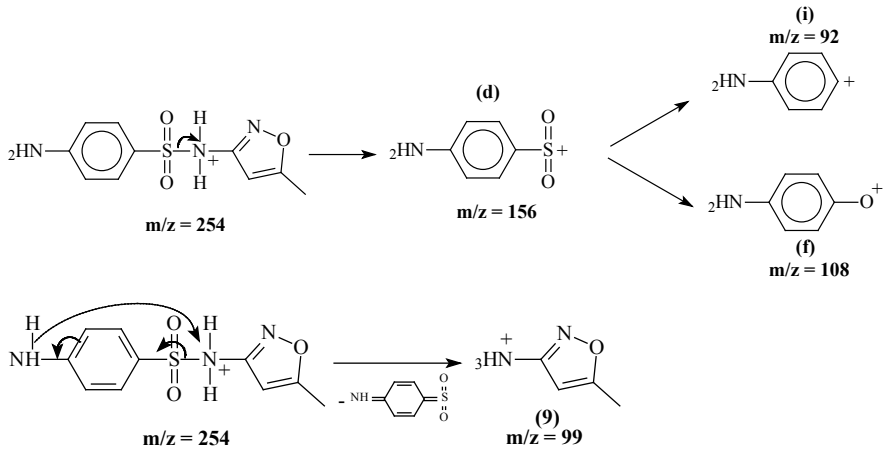

Scheme 4: Intramolecular rearrangement.

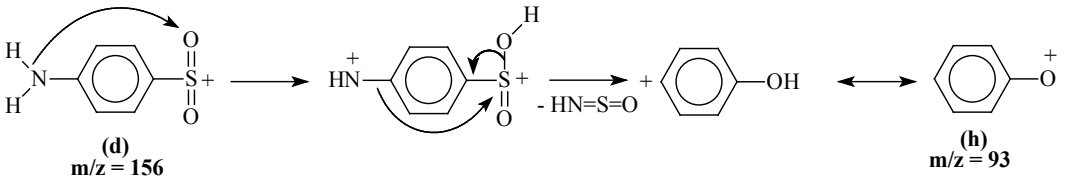

Scheme 5: Intramolecular hydrogen transfer from amine group to the SO2 group followed by the loss of neutral NH=S=O molecule.

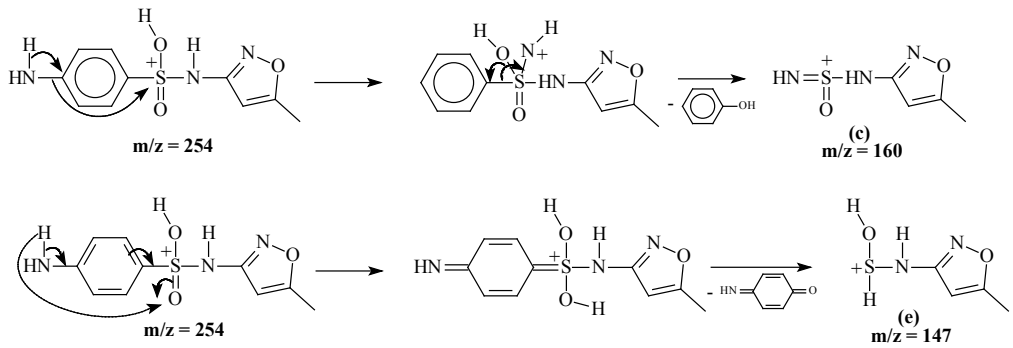

Scheme 6: The elimination of phenol and second elimination of quinine monoamine neutral molecule.

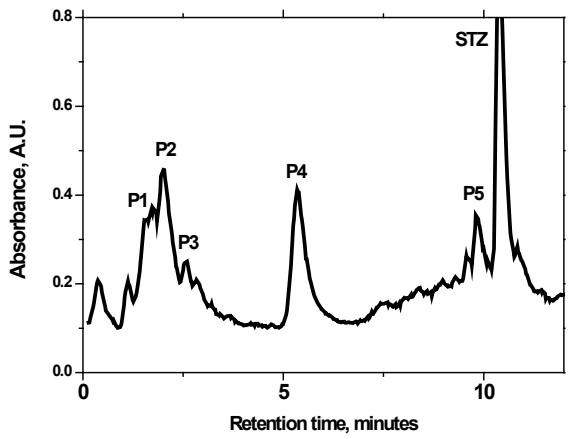

Figure 3: The Total ion chromatogram (TIC) in positive mode (ESI+) of irradiated aqueous solution of **STZ** (1.0×10^{-4} mol L^{-1}) obtained for 35% conversion. Excitation in the suntest at a pH of 5.3.

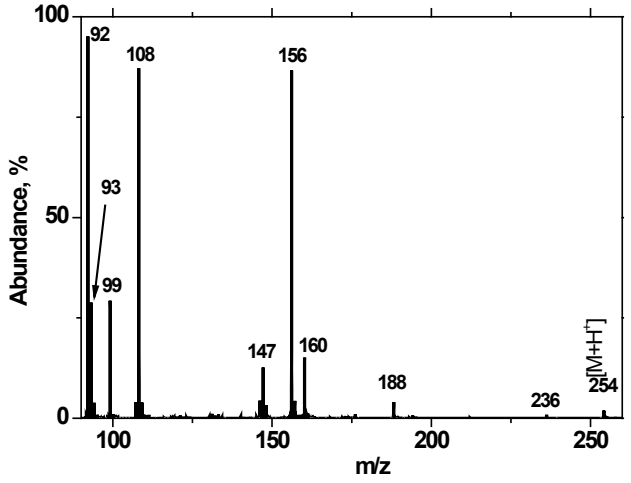

Figure 4: Collision induced dissociation spectra of [**STZ**+H]$^+$ as obtained for a collision energy of 20 eV.

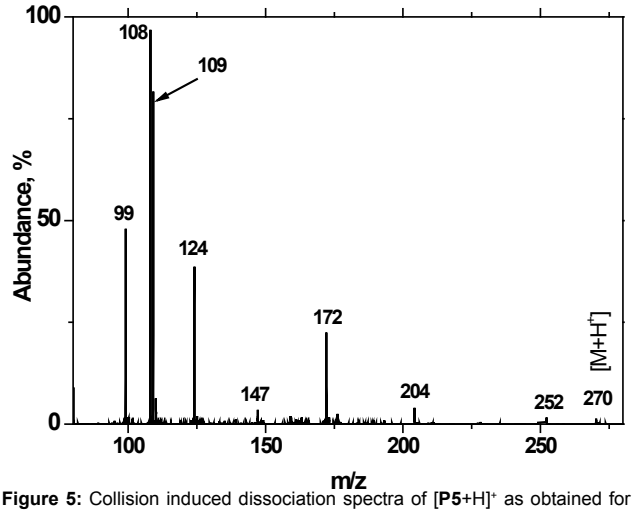

Figure 5: Collision induced dissociation spectra of [**P5**+H]$^+$ as obtained for a collision energy of 20 eV.

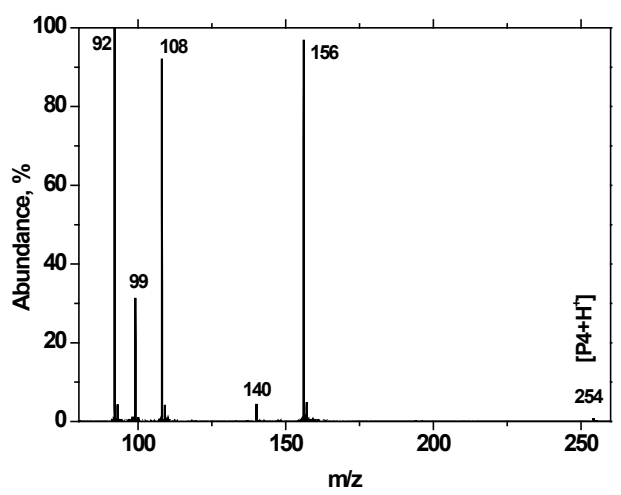

Figure 6: Collision induced dissociation spectra of [**P4**+H]$^+$ as obtained for a collision energy of 20 eV.

Fragment label	m/z	Calculated mass	Elemental composition	Accurate mass	Error (ppm)
a	236	236.0494	$C_{10}H_{10}N_3O_2S^+$	236.0508	+6.0
b	188	188.0824	$C_{10}H_{10}N_3O^+$	188.0809	-7.9
c	160	160.0181	$C_4H_6N_3O_2S^+$	160.0151	-18.6
d	156	156.0119	$C_6H_6NO_2S^+$	156.0121	+1.1
e	147	147.0228	$C_4H_7N_2O_2S^+$	147.0209	-13.1
f	108	108.0449	$C_6H_6NO^+$	108.0441	-7.8
g	99	99.0558	$C_4H_7N_2O^+$	99.0556	-2.4
h	93	93.0340	$C_6H_5O^+$	93.0324	-17.6
i	92	92.0500	$C_6H_6N^+$	92.0504	+4.1

Table 2: Accurate, exact masses and elemental composition of the fragment ions obtained from **STZ** under LC/MS^2 in ESI+ mode upon energy collision of 10 eV.

Common fragments	Specific fragments for STZ	Specific fragments for P5
99	**STZ:** 254	**P5:** 270
160	236	252
147	188	204
-	156	172
-	108	124
-	93	109
-	92	108

Table 3: Comparison of the CID spectrum of **STZ** with that of **P5**.

of molecular oxygen (Scheme 8). The role of oxygen in the process was clearly demonstrated by the increase of the quantum yield in oxygenated conditions.

Analysis of P3: The elemental composition of **P3**, $C_{10}H_{12}N_3O^+$, indicates the loss of SO_2 when compared to that of the starting compound. The small amount of such compound did not allow us to extract a well defined CID spectrum. However, the photochemical desulfonation process is largely reported in the literature [20] for similar compounds and proceeds via an intramolecular rearrangement of **STZ** excited state (Scheme 9).

CID analyses of P4: P4 gives an elemental composition ($C_{10}H_{12}N_3O_3S^+$, error=-8.4 ppm) similar to that of the starting compound leading us to the conclusion that we are dealing with an isomeric structure of **STZ**. Its CID spectrum (Figure 6) shows several fragment ions that are also present in that of **STZ,** namely m/z=92, 99, 108 and 156.

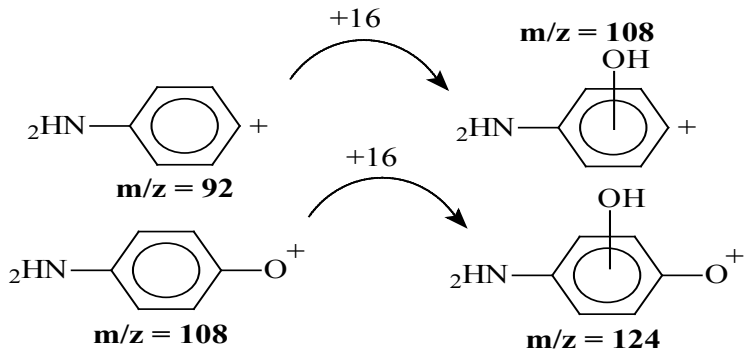

Scheme 7: Conversion of fragment ion m/z=92 and converted to m/z=108.

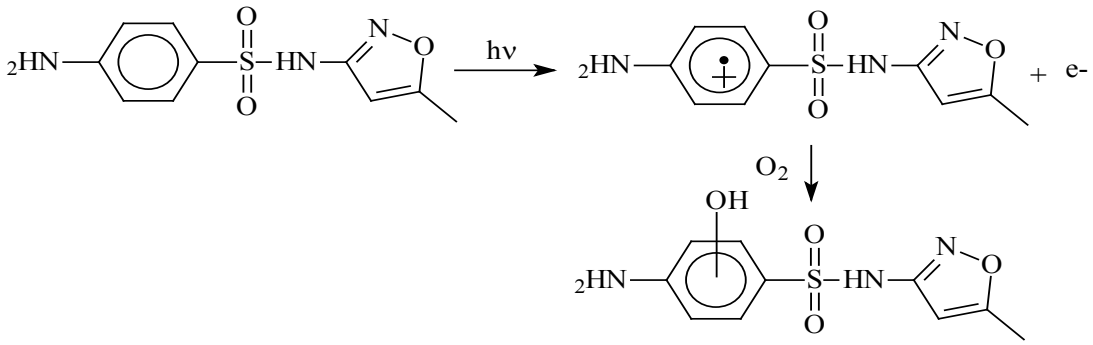

Scheme 8: Addition of oxygen atom on the phenyl moiety as a hydroxyl group.

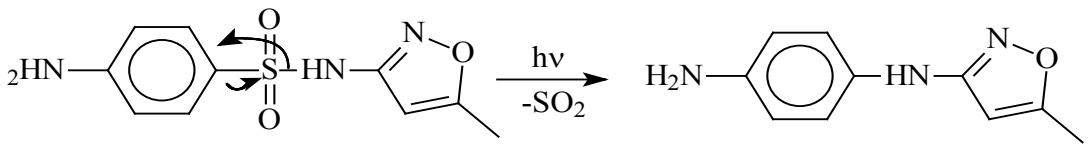

Scheme 9: Intramolecular rearrangement of STZ excited state.

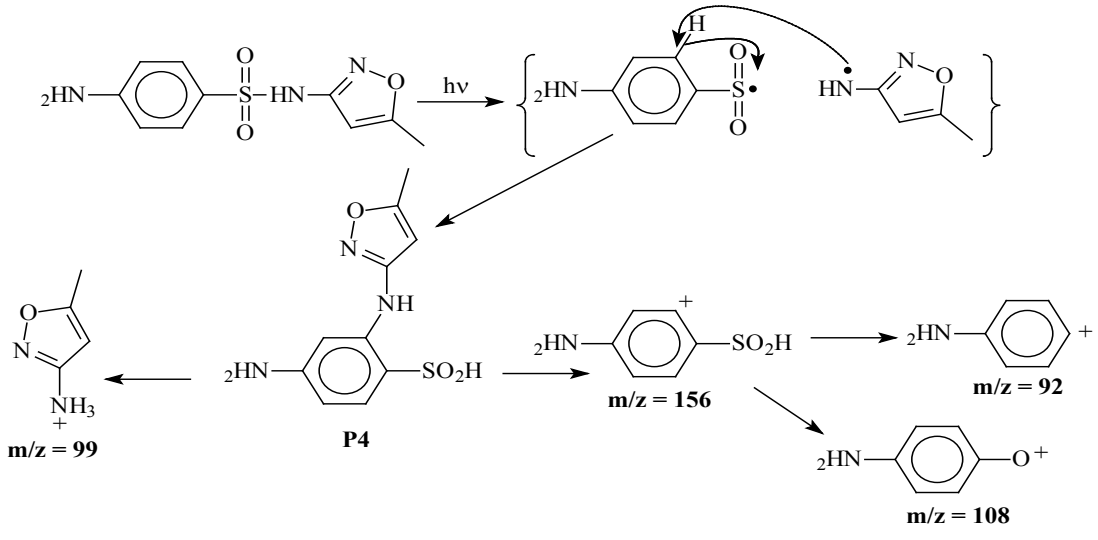

Scheme 10: Hydrogen transfer from the phenyl group leading to a chemical structure.

The possible pathway for the formation of such isomer is a Photo Fries process. It involves a homolytic scission of the S-N bond leading to the formation of a radical pair that recombines in a concerted manner after an hydrogen transfer from the phenyl group leading to a chemical structure which is in perfect agreement with the CID spectrum as shown below (Scheme 10).

Conclusion

The elucidation of the byproducts by HPLC/MS/MS generated upon solar light excitation of the antimicrobial sulfamethoxazole (**STZ**) gives evidence for the involvement of several photochemical processes. Among them, a selective hydroxylation of the phenyl group of the aniline moiety, the photoscission of the S-N bond through a photohydrolysis process, a photo Fries process that leads to an isomeric species of sulfamethoxazole and a desulfonation process.

References

1. Arántegui J, Prado J, Chamarro E, Esplugas S (1995) Kinetics of the UV degradation of atrazine in aqueous solution in the presence of hydrogen peroxide. J Photochem Photobiol 88: 65-74.
2. Floesser-Mueller H, Schwack W (2001) Photochemistry of organophosphorus insecticides. InReviews of Environmental Contamination and Toxicology 172: 129-228.
3. Hodgson E, Levi PE (1996) Pesticides: an important but underused model for the environmental health sciences. Environ Health Perspect 104 Suppl 1: 97-106.
4. Lartiges SB, Garrigues PP (1995) Degradation Kinetics of Organophosphorus and Organonitrogen Pesticides in Different Waters under Various Environmental Conditions. Environ Sci Technol 29: 1246-1254.
5. Matson PA, Parton WJ, Power AG, Swift MJ (1997) Agricultural intensification and ecosystem properties. Science 277: 504-509.
6. Zuccato E, Castiglioni S, Fanelli R, Reitano G, Bagnati R, et al. (2006) Pharmaceuticals in the environment in Italy: causes, occurrence, effects and control. Environ Sci Pollut Res Int 13: 15-21.
7. Menager M, Sarakha M (2013) Simulated solar light phototransformation of organophosphorus azinphos methyl at the surface of clays and goethite. Environ Sci Technol 47: 765-772.
8. Menager M, Siampiringue M, Sarakha M (2009) Photochemical behaviour of phenylbenzoquinone at the surface of the clays: Kaolinite, bentonite and montmorillonite. J Photochem Photobiol A: Chem 208:159-163.
9. Yuan F, Hu C, Hu X, Wei D, Chen Y, et al. (2011) Photodegradation and toxicity changes of antibiotics in UV and UV/H(2)O(2) process. J Hazard Mater 185: 1256-1263.
10. Gómez MJ, Sirtori C, Mezcua M, Fernández-Alba AR, Agüera A (2008) Photodegradation study of three dipyrone metabolites in various water systems: identification and toxicity of their photodegradation products. Water Res 42: 2698-2706.
11. Virág D, Naár Z, Kiss A (2007) Microbial toxicity of pesticide derivatives produced with UV-photodegradation. Bull Environ Contam Toxicol 79: 356-359.
12. Schwartz T, Volkmann H, Kirchen S, Kohnen W, Schön-Hölz K, et al. (2006) Real-time PCR detection of Pseudomonas aeruginosa in clinical and municipal wastewater and genotyping of the ciprofloxacin-resistant isolates. FEMS Microbiol Ecol 57: 158-167.
13. Seifrtová M, Pena A, Lino CM, Solich P (2008) Determination of fluoroquinolone antibiotics in hospital and municipal wastewaters in Coimbra by liquid chromatography with a monolithic column and fluorescence detection. Anal Bioanal Chem 391: 799-805.
14. Jiao S, Zheng S, Yin D, Wang L, Chen L (2008) Aqueous oxytetracycline degradation and the toxicity change of degradation compounds in photoirradiation process. J Environ Sci (China) 20: 806-813.
15. Braschi I, Blasioli S, Gigli L, Gessa CE, Alberti A, et al. (2010) Removal of sulfonamide antibiotics from water: Evidence of adsorption into an organophilic zeolite Y by its structural modifications. J Hazard Mater 178: 218-225.
16. García-Galán MJ, Díaz-Cruz MS, Barceló D (2008) Identification and determination of metabolites and degradation products of sulfonamide antibiotics. TrAC Trends Anal Chem 27: 1008-1022.
17. Hruska K, Franck M (2012) Sulfonamides in the environment: A review and a case report. A review and a case report Vet. Med. Czech 57: 1-35.
18. Hoseini L, Bagheri Ghomi A (2017) Photocatalytic degradaton of Sulfamethoxazole using nanosized CdO in aqueous solution. Int. J. Nano Dimens 8: 159-163.
19. Grbović G, Trebše P, Dolenc D, Lebedev AT, Sarakha M (2013) LC/MS study of the UV filter hexyl 2-[4-(diethylamino)-2-hydroxybenzoyl]-benzoate (DHHB) aquatic chlorination with sodium hypochlorite. J Mass Spectrom 48: 1232-1240.
20. Le Fur C, Legeret B, de Sainte Claire P, Wong-Wah-Chung P, Sarakha M (2013) Liquid chromatography/electrospray ionization quadrupole time-of-flight mass spectrometry for the analysis of sulfaquinoxaline byproducts formed in water upon solar light irradiation. Rapid Commun Mass Spectrom 27: 722-730.